Getting Ready for Beyond-5G, Super-IoT and 6G at Hardware Passive Components Level – A Multi-State RF-MEMS Monolithic Step Attenuator Analyzed up to 60 GHz

Jacopo Iannacci (iannacci@fbk.eu)
Fondazione Bruno Kessler https://orcid.org/0000-0001-6462-4814
Girolamo Tagliapietra
Fondazione Bruno Kessler

Research Article

Keywords: 6G, Artificial Intelligence (AI), Beyond-5G, Internet of Things (IoT), Microtechnologies, Millimeter Waves (mm-Waves), Reconfigurable RF passives, RF-MEMS, RF power step attenuator, Super-IoT, WEAF Mnecosystem.

Posted Date: November 2nd, 2021

DOI: https://doi.org/10.21203/rs.3.rs-1029005/v1

Version of Record: A version of this preprint was published at Microsystem Technologies on March 31st, 2022. See the published version at https://doi.org/10.1007/s00542-022-05285-w.

Getting Ready for Beyond-5G, Super-IoT and 6G at Hardware Passive Components Level – A Multi-State RF-MEMS Monolithic Step Attenuator Analyzed up to 60 GHz

Jacopo Iannacci[1,*], Girolamo Tagliapietra[1]

1) Fondazione Bruno Kessler – FBK,

38123, Trento – Italy

* Corresponding Author – Email: iannacci@fbk.eu; Phone: +39 0461 314 441

Abstract

Looking at 2030, the landscape of technology will be dominated by paradigms like 6G, Super-IoT (Internet of Things) and Tactile Internet (TI). From the perspective of Hardware (HW) components technologies, the turning into reality of such scenarios will demand for a radical reconceptualization of devices, sub-systems and systems, probably modifying the concept of HW itself. Driven by the target of taking initial steps in the direction of such future applications, this work discusses a 4 bit RF power step attenuator entirely realized in RF-MEMS technology. Physical samples are fabricated in a surface micromachining technology and rely on electrostatically actuated cantilevered MEMS ohmic switches to select or short resistive loads placed along the RF line. Fabricated devices are tested and validated up to 30 GHz, while simulations are discussed up to 60 GHz for the full set of allowed configurations. Despite a few technology non-idealities, the network shows levels of attenuation with a flatness as good as 1 dB over 60 GHz frequency span. The measured and simulated data reported in this work offer important indications on how to improve the network concept, both at technology and design level.

Keywords

6G, Artificial Intelligence (AI), Beyond-5G, Internet of Things (IoT), Microtechnologies, Millimeter Waves (mm-Waves), Reconfigurable RF passives, RF-MEMS, RF power step attenuator, Super-IoT, WEAF Mnecosystem.

1. Introduction

Nowadays, key application scenarios like the Internet of Things (IoT) and the Internet of Everything (IoE) turned to be so widespread, that significant part of R&D in the fields of modern electronics and Hardware (HW) technologies falls under such umbrellas, especially if looking at the area of remote and distribute smart sensing. On a different plane of reference, the 5G covers a role similar to IoT/IoE for whatever involves telecommunications and transmission of data, taking up the challenge of becoming the enabler of pervasivity of the IoT and IoE [1]. To this end, just mentioning applications like Virtual/Augmented Reality (VR/AR) and Machine-To-Machine (M2M) interaction, frames unprecedented needs in terms of mobile broadband and reliability of communications [2]–[6]. Nonetheless, despite still in the early days of its deployment, the 5G is already predicted to fail the promise of enabling the so-called Super-IoT [7],[8] and Tactile Internet (TI) [9] paradigms, shifting the attention ahead on 6G [7],[10]. This is because the 5G, although its innovations, still relies on classical HW-SW (Software) co-design approaches [11]–[13]. From a different perspective, the future 6G. also in light of massive exploitation of Artificial Intelligence (AI), will demand for more separation and symmetry between HW and SW [14]–[17], probably pushing the reformulation of the HW concept itself, as hypnotized in [18].

In light of the just sketched future scenario, this work discusses a miniaturized 4 bit, 1.4 by 1.4 mm^2 RF power step attenuator realized in RF-MEMS technology. Programmable attenuators, along with phase shifters, are key components to enable advanced beamforming of future 5G/6G antennas (e.g. massive-MIMOs), and the device here reported is tested and validated up to 60 GHz, as discussed in the next sections.

2. II. RF-MEMS Attenuator design concept

The multi-state RF power step attenuator design concept here at stake is implemented within an RF-MEMS technology platform based on a surface micromachining technology performed on 6 inch silicon wafers [19],[20]. In particular, a bank of resistive loads realized by a boron doped polycrystalline silicon layer (poly-si) is inserted on the RF line. Such resistors load the line or are selectively shorted, depending on the ON/OFF state of electrostatically driven MEMS ohmic switches. The whole RF-MEMS network is framed within the classical Coplanar Waveguide (CPW) configuration, as reported by the microphotograph in Fig. 1a.

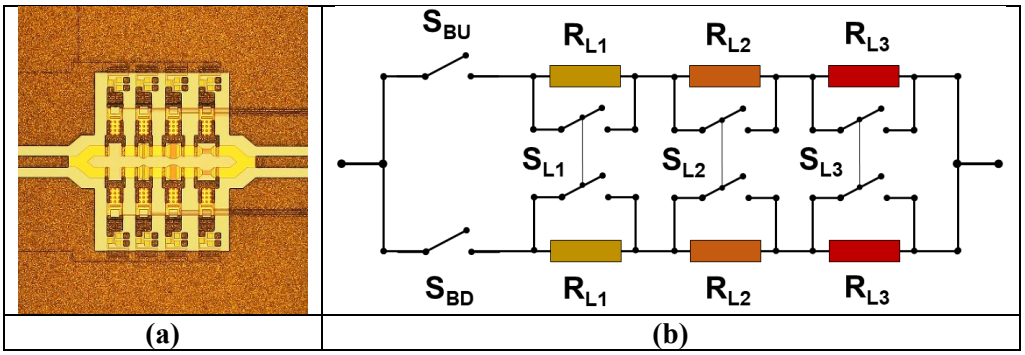

Figure 1. (a) Microphotograph of a fabricated sample of the monolithic RF-MEMS step attenuator. The footprint of the whole network is 1.4 by 1.4 mm^2. (b) Equivalent network of the intrinsic attenuator network. The resistive loads (R_{L1}, R_{L2}, R_{L3}) are deployed on two parallel branches. The independent switches S_{BU} and S_{BD} select one or both branches (or none, when the network is OPEN), while the switches S_{L1}, S_{L2} and S_{L3}, when CLOSE, short the corresponding load/loads.

The schematic in Fig. 1b summarizes how the attenuation is implemented. The RF line is split in two parallel branches, individually selected by the MEMS switches S_{BU} and S_{BD} (Switch Branch Up/Down). Then, each branch is loaded by three resistors in series, i.e. R_{L1}, R_{L2} and R_{L3}. Given that the nominal sheet resistance of the poly-si layer is 100 Ω/sq, the resistors are shaped to be 10 Ω, 40 Ω and 200 Ω, respectively.

The three resistors can be selectively shorted on both branches, when the switches S_{L1}, S_{L2} and S_{L3} are actuated. Given the just discussed configuration, the RF-MEMS step attenuator realizes 15 different levels of

attenuation, plus the THRU and OPEN configurations, when the all the switches are ON, or S_{BU} and S_{BD} are OFF, respectively. Details of the MEMS switch used in the attenuator are reported in Fig. 2.

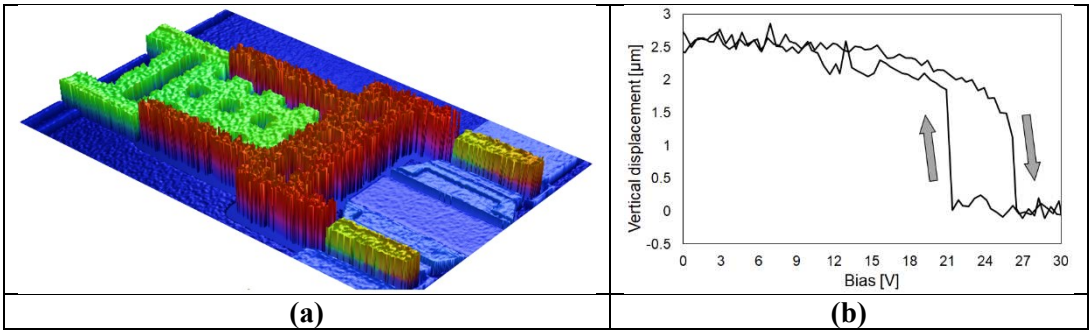

(a) **(b)**

Figure 2. (a) Experimental 3D profile of a cantilever-based MEMS series ohmic switch, measured with a white light interferometer. The color scale is related to the height along the vertical direction. (b) Experimental pull-in/pull-out characteristic of the MEMS switch.

Fig. 2a shows the 3D profile of a cantilever-based RF-MEMS series ohmic switch, like those visible in Fig. 1a. The electrostatically actuated gold membrane is hinged on one end, while it is suspended on the other. Two fingers, visible in the righthand side of Fig. 2a, short the input/out terminations of the RF line when the switch is ON. The color scale represents the vertical quote of the sample, observed with a white light interferometer. Fig. 2b reports the experimental pull-in/pull-out characteristic of the switch, in response to a triangular biasing waveform. The curve is acquired with a dynamic profiling system, and the switch exhibits an actuation and release voltages of 27 V and 21 V, respectively.

3. Experimental RF Validation and Simulations

This section focuses on the experimental characterization of the step attenuator Scattering parameters (S-parameters), as well as on the validation and simulation of a Finite Element Method (FEM) model of the device. The S-parameters are measured by means of a Vector Network Analyzer (VNA) and micro-probes on a probe station, up to 30 GHz. The VNA is calibrated with the SOLT (Short-Open-Load-Thru) method. Then, FEM simulations are performed within Ansys HFSS, relying on a full-3D model of the network in Fig. 1a.

3.1. A. Experimental Validation up to 30 GHz

Before discussing the validation, it has to be stressed that the RF-MEMS samples available for testing come from a fabricated batch exhibiting two relevant non-idealities. In the first place, the boron implanted dose was smaller than nominal. Then, the poly-si is more resistive than expected, exhibiting 250 Ω/sq instead of 100 Ω/sq, thus yielding loading resistor of 25 Ω, 100 Ω and 500 Ω.

More relevantly, an unwanted oxidation of the aluminum based underpass layer occurred in correspondence with vias openings. This leads to the presence of a thin oxide layer wherever there is a vertical transition between gold (CPW level) and the underneath aluminum (underpass). The oxide behaves as a parasitic capacitor affecting the low frequency range, and as a parasitic resistor as the frequency increases, as already observed in [19].

The HFSS 3D model is defined to account for the poly-si sheet resistance of 250 Ω/sq, however neglecting the presence of the parasitic thin-oxide where vertical vias are opened. In light of these considerations, the comparison of the measured and simulated attenuation (S21) is plotted in Fig. 3.

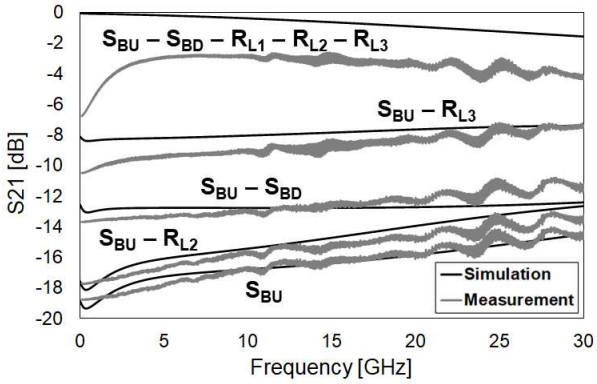

Figure 3. Comparison of the measured and simulated attenuation (S21) up to 30 GHz of the RF-MEMS in five configurations, including the THRU state (none of the resistor inserted) and the maximum attenuation (R_{L1}, R_{L2}, R_{L3} inserted and a single branch selected).

The five measured configurations include the no attenuation state (i.e. THRU), when all the switches are actuated, the maximum attenuation, when just S_{BU} is ON, plus three intermediate levels of attenuation. From a qualitative point of view, a disagreement between the measured and simulated traces is visible below 5 GHz, with the experiments showing larger attenuation, highlighting a decreasing trend as the frequency

gets higher. This is due to the parasitic capacitive behavior of the residual oxide layer of vertical vias. As the frequency increases and the parasitic capacitors start to conduct (short), the parasitic resistive contribution of such an unwanted layer kicks in, yielding additional loss over the whole range. This brings to the quantitative disagreement visible in Fig. 3, with simulations overestimating the transmission (S21), especially in the THRU state, with a constant difference of 2 dB over the whole frequency range. In light of these considerations, the HFSS model is able to produce accurate predictions of the RF-MEMS network S-parameters behavior, as emerging from the other network configurations in Fig. 3, as well.

3.2. B. Simulations up to 60 GHz

Starting from the discussion developed above, the FEM 3D model is now used to analyze the S-parameters characteristics of the RF-MEMS attenuator in all its configurations, accounting for the nominal poly-si resistivity of 100 Ω/sq. Simulations are performed up to 60 GHz, despite the validation in Fig. 3 was done just up to 30 GHz. This is a sensible choice as the same modelling approach was previously validated for similar RF-MEMS structures up to much higher frequencies [20], exhibiting accurate results. The plots in Fig. 4 report the S-parameters behavior of the attenuator in the eight resistive load configurations, when both branches are selected (S_{BU} and S_{BD} ON).

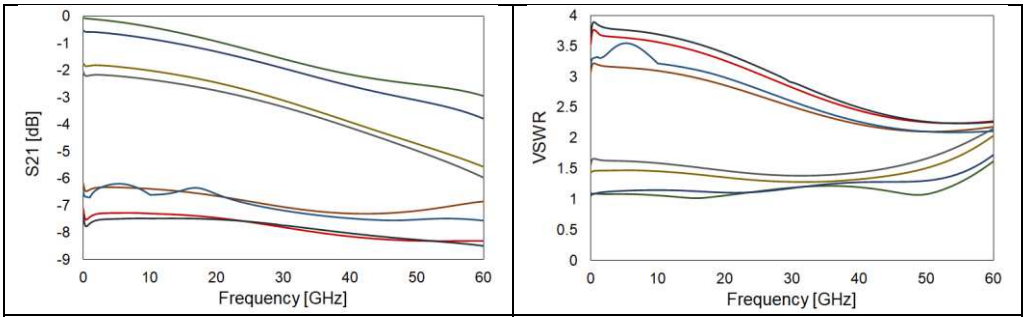

(a) **(b)**

Figure 4. Attenuation (S21) (a) and Voltage Standing Wave Ratio (VSWR) (b) simulated up to 60 GHz of the eight resistive loads combinations when both branches are selected (S_{BU} and S_{BD} ON).

Fig. 4a shows the eight attenuation (S21) levels, including the THRU state (no loads). All the traces exhibit a rather flat behavior over the wide range of 60 GHz, with a variation of about 3 dB in the worst case, and of

about 1 dB in the best case. Also relevantly, the Voltage Standing Wave Ratio (VSWR) reported in Fig. 4b has to be analyzed, since it provides important indications in terms of fractions of reflected power. To this end, if a maximum VSWR acceptable threshold is set to 2.5, corresponding to around 20% of reflected power, not all the network configurations are to be considered useful to attenuate the RF signal. In this case, just the four configurations in Fig. 4a with less attenuation are viable over the whole range, while the other four are acceptable just above 40 GHz. The other eight network configurations (S_{BU} ON and S_{BD} OFF) are shown in Fig. 5.

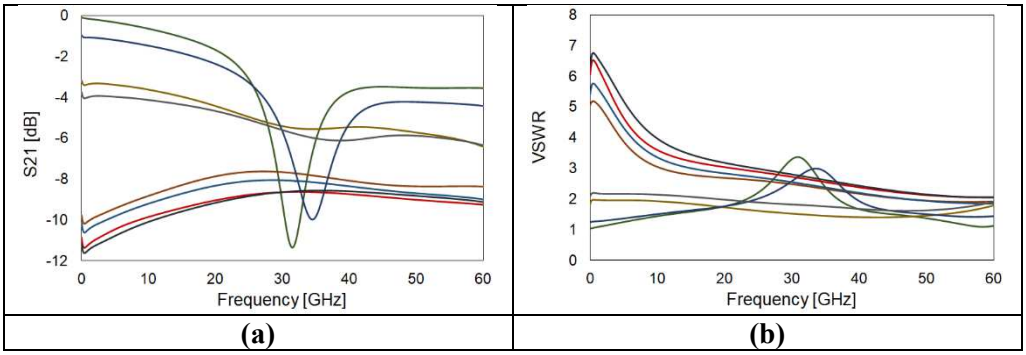

Figure 5. Attenuation (S21) (a) and VSWR (b) simulated up to 60 GHz of the eight resistive loads combinations when a single branch is selected (S_{BU} ON, S_{BD} OFF).

The larger resistive loads, due to the involvement of a single branch, yield higher attenuation levels, up to around 12 dB, as visible in Fig. 5a. The two configurations with lower attenuation show a negative peak of the S21 in the 30-40 GHz range, very likely due to the parasitic behavior of the open lower branch. Such a characteristic is not visible in the other configurations, probably because hidden by the larger signal attenuation. However, the traces not affected by the mentioned peak confirm a marked flatness of attenuation up to 60 GHz. Eventually, similar considerations to the previous ones must be developed looking the VSWR in Fig. 5b, confirming that not all the configurations can be in fact exploited to attenuate the input RF signal. The reported results, despite preliminary, offer relevant sparks on how to improve this and other RF-MEMS-based design concepts, in view of future Beyond-5G and 6G mm-Waves applications. To this end, resistive loads should be reshaped, in order to add lower and intermediated attenuation levels, thus improving the

VSWR. Also, the fact of having two branches in parallel should be perfected, in order to avoid unwanted negative resonances.

4. Conclusion

The future scenarios of Beyond-5G, 6G and Super-IoT, along with massive capitalization on Artificial Intelligence (AI), urge for radical paradigm shifts also at Hardware (HW) component level. Driven by the target of getting ready for such scenarios, this work discussed an RF-MEMS multi-state power attenuator, expected to be a key-component, together with phase shifters, for advanced beamforming capabilities. The RF behavior of the 4 bit programmable network was measured and validated up to 30 GHz, while Finite Element Method (FEM) simulations showed its full characteristics up to 60 GHz. Despite some non-idealities of technology, the network exhibited good characteristics, with flatness of attenuation (S21) as good as 1 dB over 60 GHz frequency span. The reported design concept admits margins of improvement, both at technology and design level, confirmed by the data reported and discussed in this work.

References

[1] Wei X, Shen X, Zheng K. *5G mobile communications. Berlin: Springer; 2017. 691 p.*

[2] Evolving LTE to fit the 5G future. https://www.ericsson.com/en/reports-and-papers/ericsson-technology-review/articles/evolving-lte-to-fit-the-5g-future. Accessed May 17, 2021.

[3] 5G Network Architecture a High-Level Perspective. https://www.huawei.com/minisite/hwmbbf16/insights/5G-Nework-Architecture-Whitepaper-en.pdf. Accessed May 17, 2021.

[4] The path to 5G: as much evolution as revolution. https://www.3gpp.org/news-events/3gpp-news/1774-5g_wiseharbour. Accessed May 17, 2021.

[5] Agyapong PK, Iwamura M, Staehle D, Kiess W, Benjebbour A. Design considerations for a 5G network architecture. *IEEE Commun Mag*. 2014;52(11):65-75. doi:10.1109/MCOM.2014.6957145

[6] Osseiran A, Boccardi F, Braun V, et al. Scenarios for 5G mobile and wireless communications: The vision of the METIS project. IEEE Commun Mag. 2014;52(5):26-35. doi:10.1109/MCOM.2014.6815890

[7] Zhang L, Liang YC, Niyato D. 6G Visions: Mobile ultra-broadband, super internet-of-things, and artificial intelligence. *China Commun*. 2019;16(8). doi:10.23919/JCC.2019.08.001

[8] Saad W, Bennis M, Chen M. A Vision of 6G Wireless Systems: Applications, Trends, Technologies, and Open Research Problems. *IEEE Netw*. 2020;34(3). doi:10.1109/MNET.001.1900287

[9] The Tactile Internet. https://www.itu.int/dms_pub/itu-t/oth/23/01/T23010000230001PDFE.pdf. Accessed May 17, 2021.

[10] Katz M, Matinmikko-Blue M, Latva-Aho M. 6Genesis Flagship Program: Building the Bridges Towards 6G-Enabled Wireless Smart Society and Ecosystem. In: *Proceedings - 2018 10th IEEE Latin-American Conference on Communications, LATINCOM 2018*. ; 2019. doi:10.1109/LATINCOM.2018.8613209

[11] Noguera J, Badia RM. HW/SW codesign techniques for dynamically reconfigurable architectures. *IEEE Trans Very Large Scale Integr Syst*. 2002;10(4). doi:10.1109/TVLSI.2002.801575

[12] Yeniceri R, Huner Y. HW/SW Codesign and Implementation of an IMU Navigation Filter on Zynq SoC with Linux. In: *2020 7th International Conference on Electrical and Electronics Engineering, ICEEE 2020*. ; 2020. doi:10.1109/ICEEE49618.2020.9102597

[13] Wolff C, Gorrochategui I, Bücker M. Managing large HW/SW Codesign projects. In: *Proceedings of the 6th IEEE International Conference on Intelligent Data Acquisition and Advanced Computing Systems: Technology and Applications, IDAACS'2011*. Vol 2. ; 2011. doi:10.1109/IDAACS.2011.6072907

[14] Ko B, Lee H, Son SH. GPS-Less Localization System in Vehicular Networks Using Dedicated Short Range Communication. In: *Proceedings - 2016 IEEE 22nd International Conference on Embedded and Real-Time Computing Systems and Applications, RTCSA 2016*. ; 2016. doi:10.1109/RTCSA.2016.26

[15] Makridis E, Charalambous T. Towards Robust Onboard Control for Quadrotors via Ultra-Wideband-based Localization. In: *2020 International Wireless Communications and Mobile Computing, IWCMC 2020*. ; 2020. doi:10.1109/IWCMC48107.2020.9148351

[16] Saxena S, Isukapati IK, Smith SF, Dolan JM. Multiagent Sensor Fusion for Connected & Autonomous Vehicles to Enhance Navigation Safety. In: *2019 IEEE Intelligent Transportation Systems Conference, ITSC 2019*. ; 2019. doi:10.1109/ITSC.2019.8917298

[17] Hu HC, Smith SF, Goldstein R. Cooperative Schedule-Driven Intersection Control with Connected and Autonomous Vehicles. In: *IEEE International Conference on Intelligent Robots and Systems*. ; 2019. doi:10.1109/IROS40897.2019.8967975

[18] Iannacci J. The WEAF Mnecosystem (water, earth, air, fire micro/nano ecosystem): a perspective of micro/nanotechnologies as pillars of future 6G and tactile internet (with focus on MEMS). *Microsyst Technol*. Published online 2021. doi:10.1007/s00542-020-05202-z

[19] Iannacci J, Giacomozzi F, Colpo S, Margesin B, Bartek M. A general purpose reconfigurable mems-based attenuator for radio frequency and microwave applications. In: *IEEE EUROCON 2009, EUROCON 2009*. ; 2009. doi:10.1109/EURCON.2009.5167788

[20] Iannacci J. *RF-MEMS Technology for High-Performance Passives The Challenge of 5G Mobile Applications*.; 2017. doi:10.1088/978-0-7503-1545-6